

Reduced order modeling based on POD of a parabolized Navier–Stokes equations model II: Trust region POD 4D VAR data assimilation

Juan Du^{a,c}, I.M. Navon^{b,*}, Jiang Zhu^a, Fangxin Fang^c, A.K. Alekseev^d

^a Institute of Atmospheric Physics, Chinese Academy of Sciences, Beijing 100029, China

^b Department of Scientific Computing, Florida State University, Tallahassee, FL 32306-4120, USA

^c Applied Modelling and Computation Group, Department of Earth Science and Engineering, Imperial College, Prince Consort Road, London SW7 2BP, UK

^d Moscow Institute of Physics and Technology, Moscow 141700, Russia

ARTICLE INFO

Keywords:

Parabolized Navier–Stokes (PNS)
Proper Orthogonal Decomposition (POD)
Cost functional
Ad-hoc adaptive POD 4D VAR
Trust region POD 4D VAR

ABSTRACT

A reduced order model based on Proper Orthogonal Decomposition (POD) 4D VAR (Four-dimensional Variational) data assimilation for the parabolized Navier–Stokes (PNS) equations is derived. Various approaches of POD implementation of the reduced order inverse problem are studied and compared including an ad-hoc POD adaptivity along with a trust region POD adaptivity. The numerical results obtained show that the trust region POD 4D VAR provides the best results amongst all the POD adaptive methods tested in all error metrics for the reduced order inverse problem of the PNS equations.

© 2012 Elsevier Ltd. All rights reserved.

1. Introduction

The parabolized Navier–Stokes (PNS) equations are simplified Navier–Stokes equations obtained by eliminating the streamwise second order viscous terms [1,2]. The solution can be obtained by marching in the streamwise direction (i.e. in the x direction along the surface, downstream direction) from some known initial location. Thus the x direction is taken as time and the y direction is taken as space for a two-dimensional problem, which makes the problem a one-dimensional problem in space actually.

The four-dimensional variational (4D VAR) data assimilation process seeks the minimum of a functional estimating the discrepancy between the solution of the model and the observation [3]. The derivation of the optimality system, using the adjoint model, permits us to compute a gradient which is used in the optimization.

The data assimilation problem, which is one type of inverse computational fluid dynamics (CFD) problems, is characterized by the high CPU time and memory load required for the computation of the cost functional and its gradient, as well as by the instability (due to ill-posedness) which prohibits use of Newton-type algorithms without prior explicit regularization [1]. Specifically, the computation of the gradient of the cost functional with respect to the control variables using the adjoint model requires the same computational effort as the direct model.

For the data assimilation problem of the PNS equations, the POD model reduction technique [4,5] for the introduction of the POD theory and [6–10] for the application of POD is introduced in order to improve the efficiency of the 4D VAR data assimilation process [11].

* Corresponding author. Tel.: +1 850 644 6560; fax: +1 850 644 0098.
E-mail address: inavon@fsu.edu (I.M. Navon).

Since the validity of the POD reduced order model is limited to the vicinity of the design parameters in the control parameter space, it might not be an appropriate model when the latest state is significantly different from the one on which the POD reduced order model is based. Therefore, an ‘ad-hoc’ adaptive POD 4D VAR data assimilation method [12,13,3] was implemented by updating the POD reduced order model during the optimization process.

To improve the performance of the ‘ad-hoc’ adaptive POD 4D VAR data assimilation method, the trust region POD 4D VAR data assimilation was introduced by Bergmann and Cordier [14] and Arian et al. [15]. It was applied to fluid mechanics for the first time by Fahl [16] in a flow control problem with the unsteady boundary condition being the control variables. In the data assimilation process of the PNS model, the initial condition is used as the control variable.

Combining the POD model reduction technique with the concept of the trust region optimization method [17] presents a framework for deciding when to update the POD reduced order model by projecting back to the high-fidelity model during the optimization process [18,16,15]. The limited-memory BFGS (L-BFGS) quasi Newton optimization method was used in the minimization of the cost function. Moreover, the trust region method is supported by a global convergence result that ensures the trust region iterates produced by the optimization algorithm that started at an arbitrary initial iterate, will converge to a local optimizer of the high-fidelity 4D VAR problem [19,18,16,15].

Part I of this paper relates to reduced order modeling based on POD of a PNS equations model and is focused on the POD reduced order forward model. The POD 4D VAR data assimilation process performed in this paper is based on the POD reduced order forward model. During the adaptive POD 4D VAR data assimilation process, a new set of snapshots is generated from the full forward PNS model using an updated initial condition (control variable). The reduced order forward model was then updated using the new set of snapshots.

In the present article we apply the POD method to derive a reduced order model of the data assimilation problem for the PNS equations and then introduce the POD 4D VAR adaptivity to improve the performance of the reduced order model. The trust region scheme is combined with POD 4D VAR data assimilation in order to solve the reduced order inverse problem more efficiently. To the best of our knowledge, this is a first application of the POD 4D VAR and the adaptive POD 4D VAR (the ad-hoc adaptive POD 4D VAR and the trust region POD 4D VAR) for a data assimilation problem addressing the PNS equations.

The paper is organized as follows. Section 2 presents the PNS model description along with the corresponding adjoint model of the PNS equations. Section 3 details the construction of the POD 4D VAR data assimilation model, consisting of Section 3.1 where the basic theory of the POD method is presented and Section 3.2 which illustrates the process of applying the POD method to the 4D VAR data assimilation of the inverse PNS model along with the algorithm of the ad-hoc adaptive POD 4D VAR method. Section 4 presents the classical trust region optimization method and the trust region scheme for the POD 4D VAR data assimilation. In Section 5 we present numerical results obtained comparing the performance of the POD 4D VAR, the ad-hoc adaptive POD 4D VAR and the trust region POD 4D VAR with that of the full 4D VAR for solving the inverse problem of the PNS equations. In Section 6 a summary and conclusions are provided including a discussion related to future research work.

2. PNS model description

2.1. Forward model

The two-dimensional steady supersonic laminar flow is modeled by the parabolized Navier–Stokes equations (PNS). This model is valid if the flow is supersonic along the x coordinate and the second order viscous effects along this direction are negligible, a fact which allows a rapid decrease in the computational time required to complete the calculation [20]. As a matter of fact, the x direction is taken as time and the y direction is taken as space when solving the equations numerically. The model description used here can be referred to Alekseev’s works on the PNS equations [21–23]. The following equations describe an under-expanded jet (Fig. 1).

$$\begin{cases} \frac{\partial(\rho u)}{\partial x} + \frac{\partial(\rho v)}{\partial y} = 0 \\ u \frac{\partial u}{\partial x} + v \frac{\partial u}{\partial y} + \frac{1}{\rho} \frac{\partial p}{\partial x} = \frac{1}{Re\rho} \frac{\partial^2 u}{\partial y^2} \\ u \frac{\partial v}{\partial x} + v \frac{\partial v}{\partial y} + \frac{1}{\rho} \frac{\partial p}{\partial y} = \frac{4}{3Re\rho} \frac{\partial^2 v}{\partial y^2} \\ u \frac{\partial e}{\partial x} + v \frac{\partial e}{\partial y} + (\kappa - 1)e \left(\frac{\partial u}{\partial x} + \frac{\partial v}{\partial y} \right) = \frac{1}{\rho} \left(\frac{\kappa}{RePr} \frac{\partial^2 e}{\partial y^2} + \frac{4}{3Re} \left(\frac{\partial u}{\partial y} \right)^2 \right) \\ p = \rho RT, e = C_v T = \frac{R}{(\kappa - 1)T}, (x, y) \in \Omega = (0 < x < x_{\max}, 0 < y < 1) \end{cases} \quad (2.1)$$

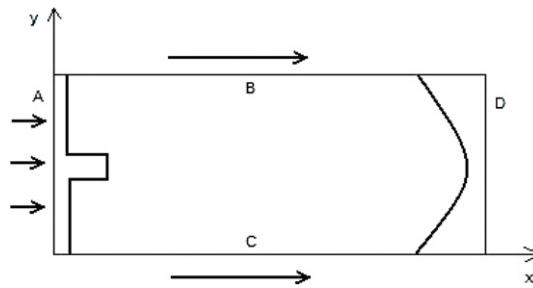


Fig. 1. Flow region. A–inflow boundary, B, C–lateral boundaries, D–outflow boundary (measurement).

where u and v represent the velocity components along the x and y directions respectively, ρ represents the flow density, p the pressure, e the specific energy, Re the Reynolds number, R the gas constant, T the temperature, C_v the specific volume heat capacity and κ is the specific heat ratio.

The following conditions are used for the inflow boundary (A, Fig. 1):

$$\rho(0, y) = \rho_\infty(y), \quad u(0, y) = u_\infty(y), \quad v(0, y) = v_\infty(y), \quad e(0, y) = e_\infty(y) \tag{2.2}$$

where $\rho_\infty(y)$, $u_\infty(y)$, $v_\infty(y)$ and $e_\infty(y)$ are all given functions.

The lateral boundary (B, C, Fig. 1) conditions are prescribed as follows:

$$\left. \frac{\partial \rho(x, y)}{\partial y} \right|_{y=0} = 0, \quad \left. \frac{\partial u(x, y)}{\partial y} \right|_{y=0} = 0, \quad \left. \frac{\partial v(x, y)}{\partial y} \right|_{y=0} = 0, \quad \left. \frac{\partial e(x, y)}{\partial y} \right|_{y=0} = 0 \tag{2.3}$$

$$\left. \frac{\partial \rho(x, y)}{\partial y} \right|_{y=1} = 0, \quad \left. \frac{\partial u(x, y)}{\partial y} \right|_{y=1} = 0, \quad \left. \frac{\partial v(x, y)}{\partial y} \right|_{y=1} = 0, \quad \left. \frac{\partial e(x, y)}{\partial y} \right|_{y=1} = 0. \tag{2.4}$$

A space-marching finite difference discretization [21] is employed in Eq. (2.5) to derive the solution of this problem. The finite difference discretization is of second order accuracy in the y direction and of first order in the x direction. At every step along the x coordinate, the flow parameters are calculated from the initial inflow location in an iterative manner assuming the form of time relaxation.

For instance, the discretization of the continuity equation assumes the following form:

$$\frac{\rho_{i,j}^{n+1} - \rho_{i,j}^n}{\tau} + u_{i,j}^n \frac{\rho_{i,j}^n - \rho_{i-1,j}^n}{\Delta x} + v_{i,j}^n \frac{\rho_{i,j+1}^{n+1} - \rho_{i,j-1}^{n+1}}{2\Delta y} + \rho_{i,j}^n \left(\frac{u_{i,j}^n - u_{i-1,j}^n}{\Delta x} + \frac{v_{i,j}^n - v_{i,j-1}^n}{\Delta y} \right) = 0 \tag{2.5}$$

where i and j denote the node index along the x and y coordinates respectively, n is the number of time iterations, and τ is the relaxation factor.

The discretization form of the other equations in (2.1) of the PNS model is obtained in a similar fashion.

2.2. Adjoint model

For the inverse problem of the PNS equations [21–23], the flow parameters $f^{\text{exp}}(x_m, y_m)$ ($m = 1, \dots, M$) at some designated points of the flow field are available. The parameters $f_{\infty(y)} = (\rho_\infty(y), u_\infty(y), v_\infty(y), e_\infty(y))$ at the entrance boundary are to be determined. In order to obtain an optimal representation of the inflow parameters, we construct a cost functional which measures the discrepancy between the measured values f^{exp} and the computed values (model predictions) with respect to the unknown parameters for a set of measurement points.

$$\epsilon(f_\infty(y)) = \sum_{m=1}^{N^0} \int_{\Omega} (f^{\text{exp}}(x, y) - f(x, y))^2 \delta(x - x_m) \delta(y - y_m) dx dy \tag{2.6}$$

where N^0 is the total number of measurement points along the x direction and $\delta(\cdot)$ is the Dirac delta function.

Using the forward model and the discrepancy functional with respect to the control variables defined above, we obtain the adjoint model corresponding to the PNS equations (2.1) as follows:

$$\left\{ \begin{aligned}
 & u \frac{\partial \Phi_\rho}{\partial x} + v \frac{\partial \Phi_\rho}{\partial y} + (\kappa - 1) \frac{\partial(\Phi_v e / \rho)}{\partial y} + (\kappa - 1) \frac{\partial(\Phi_u e / \rho)}{\partial x} - \frac{(\kappa - 1)}{\rho} \left(\frac{\partial e}{\partial y} \Phi_v + \frac{\partial e}{\partial x} \Phi_u \right) \\
 & + \left(\frac{1}{\rho^2} \frac{\partial p}{\partial x} - \frac{1}{\rho^2 Re} \frac{\partial^2 u}{\partial y^2} \right) \Phi_u + \frac{1}{\rho^2} \left(\frac{\partial p}{\partial y} - \frac{4}{3Re} \frac{\partial^2 v}{\partial y^2} \right) \Phi_v - \frac{1}{\rho^2} \left(\frac{\kappa}{RePr} \frac{\partial^2 e}{\partial y^2} + \frac{4}{3Re} \left(\frac{\partial u}{\partial y} \right)^2 \right) \Phi_e \\
 & + 2(\rho^{\text{exp}}(x, y) - \rho(x, y))\delta(x - x_m)\delta(y - y_m) = 0 \\
 & u \frac{\partial \Phi_u}{\partial x} + \frac{\partial(\Phi_u v)}{\partial y} + \rho \frac{\partial \Phi_\rho}{\partial x} - \left(\frac{\partial v}{\partial x} \Phi_v + \frac{\partial e}{\partial x} \Phi_e \right) + \frac{\partial}{\partial x} \left(\frac{P}{\rho} \Phi_e \right) + \frac{\partial^2}{\partial y^2} \left(\frac{1}{\rho Re} \Phi_u \right) \\
 & - \frac{\partial}{\partial y} \left(\frac{8}{3Re} \frac{\partial u}{\partial y} \Phi_e \right) + 2(u^{\text{exp}}(x, y) - u(x, y))\delta(x - x_m)\delta(y - y_m) = 0 \\
 & v \frac{\partial \Phi_v}{\partial y} + \frac{\partial(\Phi_v u)}{\partial x} + \rho \frac{\partial \Phi_\rho}{\partial y} - \left(\frac{\partial u}{\partial y} \Phi_u + \frac{\partial e}{\partial y} \Phi_e \right) + \frac{\partial}{\partial y} \left(\frac{P}{\rho} \Phi_e \right) \\
 & + \frac{4}{3Re} \frac{\partial^2}{\partial y^2} \left(\frac{\Phi_v}{\rho} \right) + 2(v^{\text{exp}}(x, y) - v(x, y))\delta(x - x_m)\delta(y - y_m) = 0 \\
 & \frac{\partial(u\Phi_e)}{\partial x} + \frac{\partial(v\Phi_e)}{\partial y} - \frac{(\kappa - 1)}{\rho} \left(\frac{\partial \rho}{\partial y} \Phi_v + \frac{\partial \rho}{\partial x} \Phi_u \right) - (\kappa - 1) \left(\frac{\partial u}{\partial x} + \frac{\partial v}{\partial y} \right) \Phi_e \\
 & + (\kappa - 1) \frac{\partial \Phi_v}{\partial y} + (\kappa - 1) \frac{\partial \Phi_u}{\partial x} + \frac{\kappa}{RePr} \frac{\partial^2}{\partial y^2} \left(\frac{\Phi_e}{\rho} \right) \\
 & + 2(e^{\text{exp}}(x, y) - e(x, y))\delta(x - x_m)\delta(y - y_m) = 0.
 \end{aligned} \right. \tag{2.7}$$

The boundary conditions at the outflow location D ($x = x_{\text{max}}$, Fig. 1) are

$$\Phi_\rho(x_{\text{max}}, y) = 0, \quad \Phi_u(x_{\text{max}}, y) = 0, \quad \Phi_v(x_{\text{max}}, y) = 0, \quad \Phi_e(x_{\text{max}}, y) = 0. \tag{2.8}$$

The boundary conditions applied at B ($y = 1$) and C ($y = 0$) are as follows

$$\left. \frac{\partial \Phi_\rho}{\partial y} \right|_{y=0} = 0, \quad \left. \frac{\partial \Phi_u}{\partial y} \right|_{y=0} = 0, \quad \left. \frac{\partial \Phi_v}{\partial y} \right|_{y=0} = 0, \quad \left. \frac{\partial \Phi_e}{\partial y} \right|_{y=0} = 0 \tag{2.9}$$

$$\left. \frac{\partial \Phi_\rho}{\partial y} \right|_{y=1} = 0, \quad \left. \frac{\partial \Phi_u}{\partial y} \right|_{y=1} = 0, \quad \left. \frac{\partial \Phi_v}{\partial y} \right|_{y=1} = 0, \quad \left. \frac{\partial \Phi_e}{\partial y} \right|_{y=1} = 0. \tag{2.10}$$

The gradient of the cost functional with respect to the control variables is determined by the forward model flow parameters as well as the adjoint parameters:

$$\begin{aligned}
 \frac{\partial \epsilon}{\partial e_\infty(y)} &= \Phi_e u + (\kappa - 1) \Phi_u \\
 \frac{\partial \epsilon}{\partial \rho_\infty(y)} &= \Phi_\rho u + \frac{(\kappa - 1) \Phi_u e}{\rho} \\
 \frac{\partial \epsilon}{\partial u_\infty(y)} &= \Phi_u u + \rho \Phi_p + (\kappa - 1) \Phi_e e \\
 \frac{\partial \epsilon}{\partial v_\infty(y)} &= \Phi_v u.
 \end{aligned} \tag{2.11}$$

Note that the underlying numerical procedure for the forward problem (as described in Section 2.1) is only first order accurate in the x direction. A more advanced numerical scheme is still in development. Because our purpose is to test the application of the model reduction technique to the data assimilation process, we start with the 2D PNS equations and a space-marching finite difference scheme. The x direction is taken as time and the y direction is taken as space when solving the 2D PNS equations numerically. For the space-marching finite difference scheme we adopted here, the stability can be guaranteed with first order accuracy in the x direction (taken as time).

3. POD 4D VAR

Proper Orthogonal Decomposition (POD) is a model reduction technique which provides a useful tool for efficiently approximating a large amount of data and representing fluid flows with a reduced number of degrees of freedom. We apply this method to obtain a reduced order model of the inverse problem for the PNS equations. A decrease both in CPU time and in the memory requirement is yielded for the computation of the gradient of the cost functional with respect to the control variables. A reduction in the number of optimization iterations in the reduced order 4D VAR data assimilation process is also obtained.

3.1. Proper orthogonal decomposition

Let V represent the model variables (e.g. u, v, e, p). The ensemble of snapshots sampled at designated time steps $\{V^l\}_{l=1}^L = \{V_i^l\}_{i=1}^M$ ($1 \leq i \leq M$) ($L \leq N$) can be expressed as the following $M \times L$ matrix A_V , where M is the number of nodes, N is the number of time steps, and L is the number of snapshots, respectively.

$$A_V = \begin{pmatrix} V_1^1 & V_1^2 & \dots & V_1^L \\ V_2^1 & V_2^2 & \dots & V_2^L \\ \vdots & \vdots & \vdots & \vdots \\ V_M^1 & V_M^2 & \dots & V_M^L \end{pmatrix}. \tag{3.1}$$

The average of the ensemble of snapshots $\{\bar{V}_i\}_{i=1}^M$ is defined as

$$\bar{V}_i = \frac{1}{L} \sum_{l=1}^L V_i^l, \quad 1 \leq i \leq M. \tag{3.2}$$

Taking the deviation from the mean of the variables yields

$$\widehat{V}_i^l = V_i^l - \bar{V}_i, \quad 1 \leq i \leq M, 1 \leq l \leq L \tag{3.3}$$

which constructs an $M \times L$ matrix $A = \{\widehat{V}^l\}_{l=1}^L$.

The essence of the POD method is to find a set of orthogonal basis functions $\{\phi_i\}$ ($i = 1, \dots, L$) to maximize the following representation

$$\frac{1}{L} \sum_{i=1}^L |\langle \widehat{V}^i, \phi_i \rangle_{L^2}|^2 \tag{3.4}$$

subject to

$$\langle \phi_i, \phi_j \rangle_{L^2} = 1, \quad i = j \tag{3.5}$$

$$\langle \phi_i, \phi_j \rangle_{L^2} = 0, \quad i \neq j \tag{3.6}$$

where $i, j = 1, 2, \dots, L$ and the inner product is defined in the L^2 space as $\langle f, g \rangle_{L^2} = \int_{\Omega} fgd\Omega$ in which f and g are two real functions defined on the measure space Ω .

Using the L^2 inner product, the above optimization problem becomes

$$\max_{\phi_i \in L^2} \frac{1}{L} \sum_{i=1}^L |\langle \widehat{V}^i, \phi_i \rangle_{L^2}|^2 = \max_{\phi_i \in L^2} \frac{1}{L} \sum_{i=1}^L \int_{\Omega} \widehat{V}^i \phi_i d\Omega. \tag{3.7}$$

Since the basis functions can be represented as the linear combination of the solution snapshots:

$$\phi = \sum_{i=1}^L a_i \widehat{V}^i \tag{3.8}$$

the optimization problem changes to the following eigenvalue problem

$$Cx = \lambda x \tag{3.9}$$

where

$$C = \{c_{i,j}\}_{i,j=1}^M = \left\{ \int_{\Omega} (\widehat{V}^i)^T \widehat{V}^j d\Omega \right\}_{i,j=1}^M = AA^T. \tag{3.10}$$

In order to solve the above eigenvalue problem, we employ the Singular Vector Decomposition (SVD) method to obtain an optimal representation for A [24,25], which is an important tool to construct optimal basis of reduced order approximation. For matrix $A \in R^{M \times L}$, there exists the SVD

$$A = U \begin{pmatrix} S & 0 \\ 0 & 0 \end{pmatrix} W^T \tag{3.11}$$

where $U \in R^{M \times M}$ and $W \in R^{L \times L}$ are all orthogonal matrices, $S = \text{diag}\{\sigma_1, \sigma_2, \dots, \sigma_{\ell}\} \in R^{\ell \times \ell}$ is a diagonal matrix corresponding to A , and σ_i ($i = 1, 2, \dots, \ell$) are positive singular values where ℓ denotes the number of positive singular values. The matrices $U = (\phi_1, \phi_2, \dots, \phi_M) \in R^{M \times M}$ and $W = (\varphi_1, \varphi_2, \dots, \varphi_L) \in R^{L \times L}$ contain the orthogonal eigenvectors to the AA^T and $A^T A$, respectively. The columns of these eigenvector matrices are organized corresponding to the singular

values σ_i which are comprised in \mathbf{S} in a descending order. Since the number of mesh points is much larger than that of transient points, i.e., $M \gg L$, the order M of the matrix $\mathbf{A}\mathbf{A}^T$ is also much larger than the order L of the matrix $\mathbf{A}^T\mathbf{A}$, however, their null eigenvalues are identical.

Therefore, we may first solve the eigenvalue equation corresponding to the matrix $\mathbf{A}^T\mathbf{A}$ to find the eigenvectors ϕ_j ($j = 1, 2, \dots, \ell$),

$$\mathbf{A}^T\mathbf{A}\phi_j = \lambda_i\phi_j, \quad j = 1, 2, \dots, \ell. \tag{3.12}$$

Since the singular values of the SVD method are associated with the eigenvalues of the matrices $\mathbf{A}\mathbf{A}^T$ and $\mathbf{A}^T\mathbf{A}$ in such a manner that $\lambda_i = \sigma_i^2$ ($i = 1, 2, \dots, \ell$), we may obtain ℓ ($\ell \leq L$) eigenvectors $\{\phi_j\}_{j=1}^\ell$ corresponding to the non-null eigenvalues for the matrix $\mathbf{A}\mathbf{A}^T$ by

$$\phi_j = \frac{1}{\sigma_j}\mathbf{A}\phi_j, \quad j = 1, 2, \dots, \ell \tag{3.13}$$

which can generate a space \mathcal{V} defined by $\mathcal{V} = \text{span}\{\phi_1, \dots, \phi_\ell\}$.

We have to choose an optimal subspace of dimension m given by $\mathcal{V}_m = \text{span}\{\phi_1, \dots, \phi_m\}$ to get a good approximation of the data set. The vectors ϕ_i ($i = 1, \dots, m$) are then called POD modes. The goal is to choose m small enough that the relative information content [26,27], also usually referred to as ‘energy’ $I(m)$ is near to one, which is defined by

$$I(m) = \frac{\sum_{i=1}^m \lambda_i}{\sum_{i=1}^\ell \lambda_i} \tag{3.14}$$

i.e., if the subspace \mathcal{V}_m should contain a percentage γ of the information in \mathcal{V} , then one should choose m such that [28]

$$m = \text{argmin} \left\{ I(m) : I(m) \geq \frac{\gamma}{100} \right\}. \tag{3.15}$$

In many applications like fluid dynamics, one observes an exponential decrease of the eigenvalues, so that there is a good chance to derive low-order approximate models.

Hence, the state variable can be represented by the linear combination of the retained POD basis functions as follows:

$$V(x, y) = \bar{V} + \sum_{i=1}^m \alpha_i(x)\phi_i(y) \tag{3.16}$$

where $\alpha_i(x)$ ($i = 1, \dots, m$) are the POD coefficients corresponding to every POD basis function. Note that the x direction is taken as time and the y direction is taken as space in the PNS model.

3.2. POD 4D VAR

The aim of 4D VAR data assimilation is to reconcile observations with model predictions subject to the model serving as a strong constraint [29,30]. In the full high-fidelity nonlinear 4D VAR, this process is implemented by minimizing the following cost functional with respect to the control variables:

$$J(V_0) = (V_0 - V^b)^T B^{-1} (V_0 - V^b) + \sum_{k=1}^{N^o} (H_k V_k - V_k^o)^T O^{-1} (H_k V_k - V_k^o) \tag{3.17}$$

where V_0 is the control vector, V^b is the vector containing the background information, B is the background error covariance matrix, H is an observation operator, V_k is the vector of the model prediction obtained from the full forward model, V_k^o is the observation information vector, O is the observation error covariance matrix and N^o is the number of observations taken. In the data assimilation process of the PNS model, we just consider the observation information at the outflow boundary and don't involve the background information.

The POD reduced order cost functional in POD 4D VAR assumes the form

$$J^{\text{POD}}(V_0) = (V_0^{\text{POD}} - V^b)^T B^{-1} (V_0^{\text{POD}} - V^b) + \sum_{k=1}^{N^o} (H_k V_k^{\text{POD}} - V_k^o)^T O^{-1} (H_k V_k^{\text{POD}} - V_k^o) \tag{3.18}$$

where V_0^{POD} is the reduced order control vector and V_k^{POD} is the model prediction obtained from the POD reduced order forward model.

In explicit form, the reduced order control vector and the model prediction can be represented as

$$V_0^{\text{POD}} = V_0^{\text{POD}}(0, y) = \bar{V} + \sum_{i=1}^m \alpha_i(0) \phi_i(y) \quad (3.19)$$

$$V_k^{\text{POD}} = V_k^{\text{POD}}(x_k, y) = \bar{V} + \sum_{i=1}^m \alpha_i(x_k) \phi_i(y) \quad (3.20)$$

where x_k ($k = 1, \dots, N^o$) are the locations along the x direction (playing the role of time evolution in the PNS model) where the measurements are taken and m is the number of retained POD basis functions. And $\alpha_i(x_k)$ ($i = 1, \dots, m$) are obtained from the POD reduced order forward model.

Hence, in POD 4D VAR, the control variables are $\alpha_1(0), \dots, \alpha_m(0)$. Because $m \ll N \ll M$ (N being the number of time steps, i.e. the number of nodes along the x direction, and M the number of nodes along the y direction), the dimension of the POD reduced order space is much smaller than that of the full space.

In the process of minimizing the cost functional with respect to the control variables, the limited-memory BFGS (L-BFGS) quasi-Newton method [17] is applied. The gradient of the reduced cost functional (3.18) with respect to the control variables can be expressed as

$$\nabla_{\alpha(0)} J^{\text{POD}} = \Phi^T (\nabla_{V_0} J)|_{V_0 = \bar{V} + \phi_{\alpha(0)}} \quad (3.21)$$

where $\alpha(0) = (\alpha_1(0), \dots, \alpha_m(0))^T \in R^m$ and $\Phi = (\phi_1, \dots, \phi_m) \in R^{M \times m}$ (M is the number of nodes along the y direction).

Consequently, computational savings are mainly achieved by a drastic reduction in the number of iterations due to the low dimension of the optimization problem [31].

Since the validity of the POD reduced order model is limited to the vicinity of the design parameters in the control parameter space, it might not be an appropriate model when the latest state is significantly different from the one on which the POD reduced order model is based. Therefore, an ‘ad-hoc’ adaptive POD 4D VAR algorithm [12,13,3] is proposed as follows:

- (1) Generate a set of snapshots from the solution of the full forward model using the specific control variables and construct the POD reduced order model.
- (2) Perform iterations for the optimization problem using the reduced order model with the L-BFGS method and calculate the cost functional J_n where n is the number of L-BFGS optimization iterations taken.
- (3) Check the value of the cost functional.

If $|J_n| < \epsilon$ where ϵ is the tolerance for the optimization, then stop, the POD 4D VAR data assimilation is completed;

If $|J_n| > \epsilon$ and $|J_n - J_{n-1}| > \eta$ ($\eta > 0$), then set $n = n + 1$ and go back to (2);

If $|J_n| > \epsilon$ and $|J_n - J_{n-1}| < \eta$, project back the reduced order control variables from the latest optimization iteration to the original space, generate a new set of snapshots by integrating the original forward model using the projected control variables and construct a new POD reduced order model, then go to (1).

4. The trust region POD approach

In the POD 4D VAR data assimilation, the POD reduced order model is based on the solution of the full model with the specific control variables, i.e., whose validity is limited to the vicinity of the design parameters in the control parameter space [14]. Thus it is necessary to reconstruct the POD reduced order model using a new set of snapshots generated by the original forward model when the control variables from the latest optimization iteration are significantly different from the ones on which the POD reduced order model is based. It is important to determine when to project back to the high-fidelity model and reconstruct a new POD reduced order model based on freshly derived snapshots. The trust region scheme is then applied to the POD 4D VAR data assimilation process in order to determine when to update the POD reduced order model during the optimization process. The trust region POD approach was introduced by Fahl [16] and used in fluid mechanics for the first time in [14].

4.1. Trust region method

The classical trust region method aims to define a region around the current iterate within which it trusts the model to be an adequate representation of the objective function f , and then choose the step to be the approximate minimizer of the model inside the trust region. The objective function is approximated with a model function (usually a quadratic function) only in a certain region (the so-called trust region) [17]. It is assumed that the first two terms of the approximate quadratic model function m_k at each iterate x_k are identical to the first two terms of the Taylor-series expansion of f around x_k with a step p as follows:

$$m_k(x_k + p) = f_k + \nabla f_k^T p + \frac{1}{2} p^T \mathbf{B}_k p \quad (4.1)$$

where $f_k = f(x_k)$, $\nabla f_k = \nabla f(x_k)$ and \mathbf{B}_k is an approximation to the Hessian matrix.

We solve the following constrained optimization problem of the approximate model to obtain a proper step p_k for the objective function

$$\begin{aligned} \min m_k(x_k + p) &= f_k + \nabla f_k^T p + \frac{1}{2} p^T \mathbf{B}_k p \\ \text{subject to } \|p\| &\leq \delta_k \end{aligned} \tag{4.2}$$

where δ_k is the trust region radius.

In order to choose the trust region radius δ_k at each iteration, we define the ratio

$$\rho_k = \frac{f(x_k) - f(x_k + p_k)}{m_k(x_k) - m_k(x_k + p_k)}. \tag{4.3}$$

If the ratio ρ_k is negative, the new objective value is greater than the current value so that the step p_k must be rejected. On the other hand, if ρ_k is close to 1, there is a good agreement between the approximate model m_k and the objective function f_k over this step, so it is safe to accept the step p_k and to expand the trust region radius for the next iteration. If ρ_k is positive but not close to 1, we accept this step but keep the trust region radius unchanged. But if ρ_k is positive and far from 1, this step must be rejected and the trust region radius should be shrunk.

4.2. Trust region POD 4D VAR

In order to decide when to project back to the high-fidelity model and to construct a new POD reduced order model using the updated control variables from the optimization iterations, we combine the trust region method with the POD 4D VAR data assimilation (using the trust regional adaptive POD approach).

An outline of the trust region POD 4D VAR algorithm is as follows [15,32].

Let $V^0 = V_0, \delta^0, 0 < \eta_1 < \eta_2 < 1$ and $0 < \gamma_1 < \gamma_2 < 1 < \gamma_3$ be given, set $k = 0$.

1. Generate snapshots corresponding to the control V^k using the full forward model and construct the POD reduced order model.
2. Minimize the reduced order cost functional within the trust region

$$s^k = \arg \min_{\|s\| \leq \delta^k} m^k(V^k + s). \tag{4.4}$$

3. Compute the full order model cost functional $J(V^k + s^k)$ and the ratio

$$\rho^k = \frac{J(V^k) - J(V^k + s^k)}{m^k(V^k) - m^k(V^k + s^k)}. \tag{4.5}$$

4. Update the radius of the trust region:

If $\rho^k \geq \eta_2$, set $V^{k+1} = V^k + s^k$ and increase the trust region radius $\delta^{k+1} = \gamma_3 \delta^k$, set $k = k + 1$ and GOTO 1.

If $\eta_1 < \rho^k < \eta_2$, set $V^{k+1} = V^k + s^k$ and decrease the trust region radius $\delta^{k+1} = \gamma_2 \delta^k$, set $k = k + 1$ and GOTO 1.

If $\rho^k \leq \eta_1$, set $V^{k+1} = V^k$ and decrease the trust region radius $\delta^{k+1} = \gamma_1 \delta^k$, set $k = k + 1$ and GOTO 2.

For the constrained minimization sub-problem

$$\begin{aligned} \min m^k(V^k + s) \\ \text{subject to } \|s\| &\leq \delta^k \end{aligned} \tag{4.6}$$

we use the bound-constrained L-BFGS-B algorithm [33,34]. It is not necessary to obtain the optimal solution of this problem, rather it is sufficient to compute a trial step s_k that achieves only a certain level of decrease for the full model, to start the trust region procedure. The trust region methodology is advantageous since we have rigorous convergence results [19,16] that guarantee that the trust region POD algorithm will converge to the local minimizer of the original high-fidelity optimization problem [18,16,15].

5. Numerical results

In this section, the flow-field is computed by marching along the x coordinate which is a proxy for the time evolution from $x = 0$ to $x = x_{\max}$ and in the reverse direction for the adjoint model.

5.1. Numerical results of POD 4D VAR

Let the length of the x direction of the flow-field be normalized to 1. The computational grid contains 100 points in the marching direction (the x direction) and 100 points in the transversal direction (the y direction). Set $Re = 10^3$. The measurement (observation) is taken at the outflow boundary. Fig. 2 shows the initial specific energy e of the flow at the

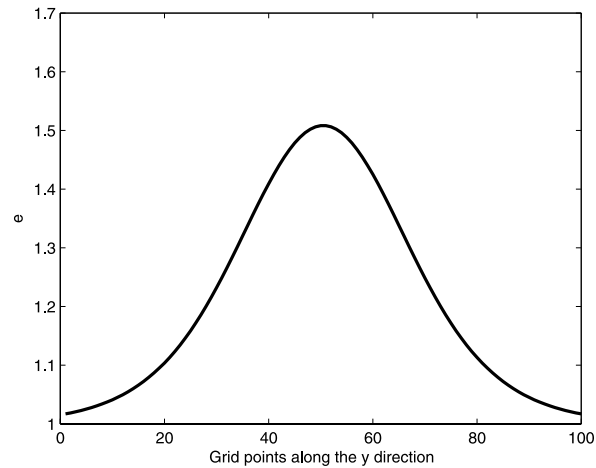


Fig. 2. The initial condition for the specific energy e at the inflow boundary A (see Fig. 1).

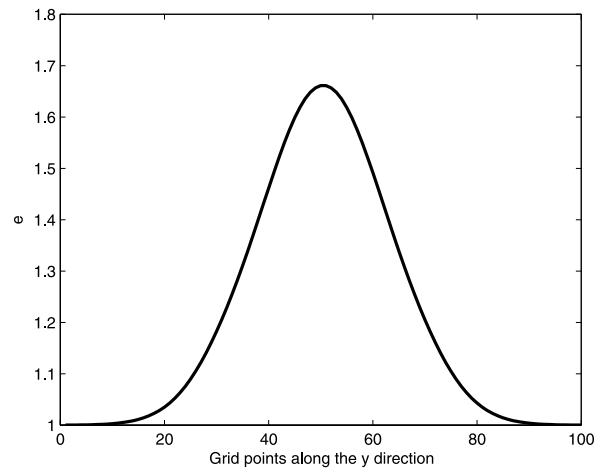


Fig. 3. The observation for the specific energy e at the outflow boundary D (see Fig. 1).

entrance boundary A ($x = 0$, Fig. 1), which was obtained using the logistic function. The observation information for the specific energy e at the outflow boundary D (see Fig. 1) is presented in Fig. 3.

The control variables, i.e., the initial condition at the entrance boundary in this case, after the full 4D VAR data assimilation compared with the exact initial condition are presented in Fig. 4.

The parameters used in the ad-hoc adaptive POD 4D VAR are taken as $\epsilon = 10^{-6}$ and $\eta = 10^{-3}$. Six POD basis functions were chosen to construct the reduced order model. The optimal initial conditions at the entrance boundary obtained by the POD 4D VAR data assimilation and the ad-hoc adaptive POD 4D VAR data assimilation as compared with the exact initial condition are presented in Fig. 5.

For the POD reduced order model, the number of POD bases $m = 6$ was chosen to maintain a 99% of energy as stated in Eq. (3.15). In Fig. 6, the reduction of the cost functional using the POD 4D VAR and the ad-hoc adaptive POD 4D VAR is compared with the result obtained using the full 4D VAR of the PNS model. It can be seen that the cost functional was reduced from an initial value 1.0 to 10^{-4} using the full 4D VAR of the PNS model. However, the POD 4D VAR and the ad-hoc adaptive POD 4D VAR can only reduce the cost functional to $10^{-1.2}$ and $10^{-1.5}$, respectively.

5.2. Numerical results of trust region POD 4D VAR

For the present case, the cost functional is chosen as follows:

$$J(e_\infty) = \sum_{n=1}^M (e^{\text{exp}}(x_{\text{max}}, y_n) - e(x_{\text{max}}, y_n))^2 \quad (5.1)$$

where M denotes the number of nodes along the y direction.

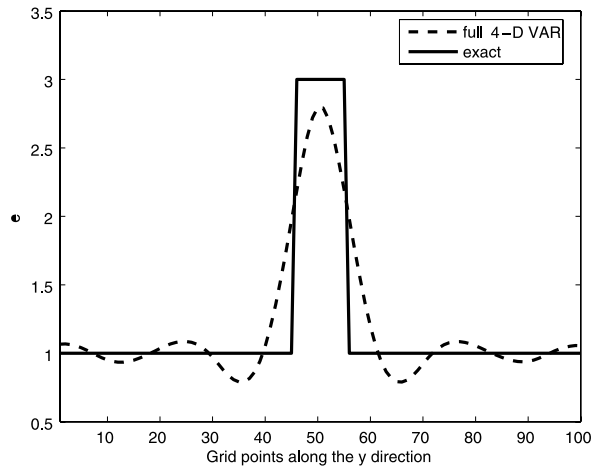


Fig. 4. The control variables at the entrance boundary for full 4D VAR data assimilation compared with the exact one.

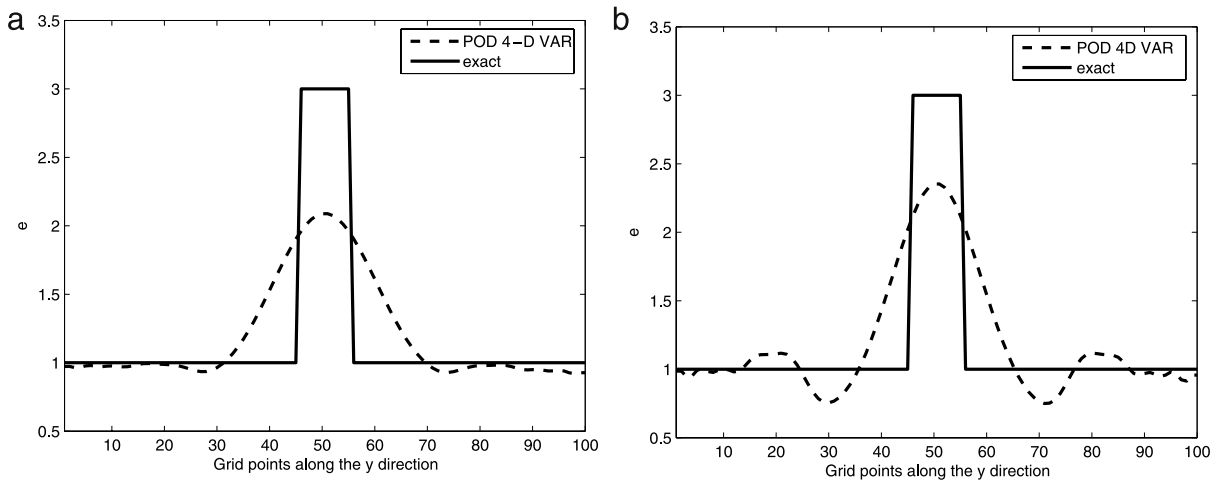


Fig. 5. The control variables at the entrance boundary for POD 4D VAR and ad-hoc adaptive POD 4D VAR compared with the exact one.

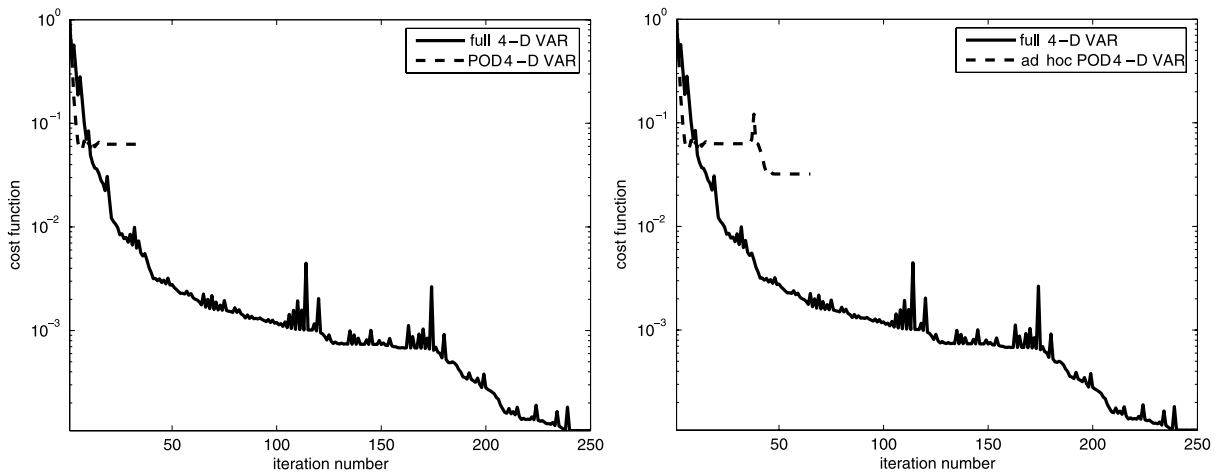


Fig. 6. The performance of minimization of the cost functional for POD 4D VAR and ad-hoc adaptive POD 4D VAR compared with full 4D VAR.

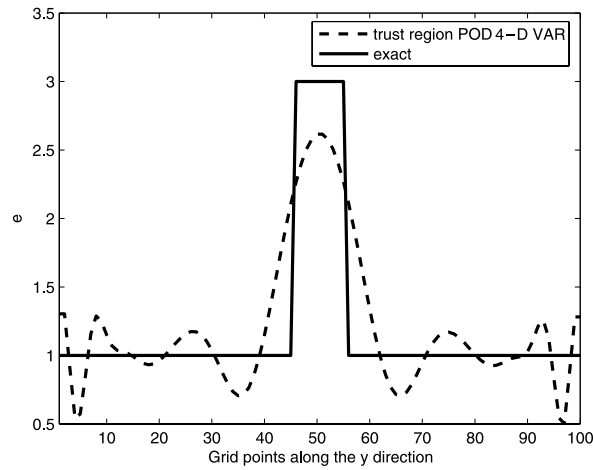


Fig. 7. The control variables at the entrance boundary for the trust region POD 4D VAR compared with the exact one.

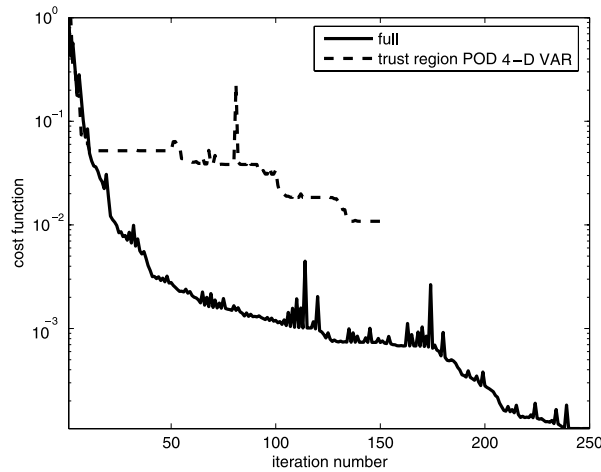


Fig. 8. The performance of minimization of the cost functional for the trust region POD 4D VAR and full 4D VAR.

In POD 4D VAR, we look for an optimal solution of the POD reduced cost function

$$J^{\text{POD}}(\alpha(0)) = \sum_{n=1}^M (e^{\text{exp}}(x_{\text{max}}, y_n) - e^{\text{POD}}(x_{\text{max}}, y_n))^2 \tag{5.2}$$

where $\alpha(0) = (\alpha_1(0), \dots, \alpha_m(0))^T$ and

$$e^{\text{POD}}(x_{\text{max}}, y) = \bar{e} + \sum_{i=1}^m \alpha_i(x_{\text{max}}) \phi_i(y) \tag{5.3}$$

where \bar{e} is the mean value of the forward model solution of the specific energy e over the time (the x direction) and ϕ_i ($i = 1, \dots, m$) are POD basis functions.

The parameters for the trust region POD 4D VAR algorithm are chosen as [16,14] $\eta_1 = 0.25, \eta_2 = 0.75, \gamma_1 = 0.25, \gamma_2 = 0.75, \gamma_3 = 2$.

In Fig. 7, the initial condition of the specific energy e at the entrance boundary after applying the trust region POD 4D VAR data assimilation is compared with the exact initial condition. The reduction of the cost functional using the trust region POD 4D VAR data assimilation compared with the one using the full 4D VAR is presented in Fig. 8, in which we can see that the cost functional was reduced from 1.0 to $10^{-1.9}$ using the trust region POD 4D VAR data assimilation.

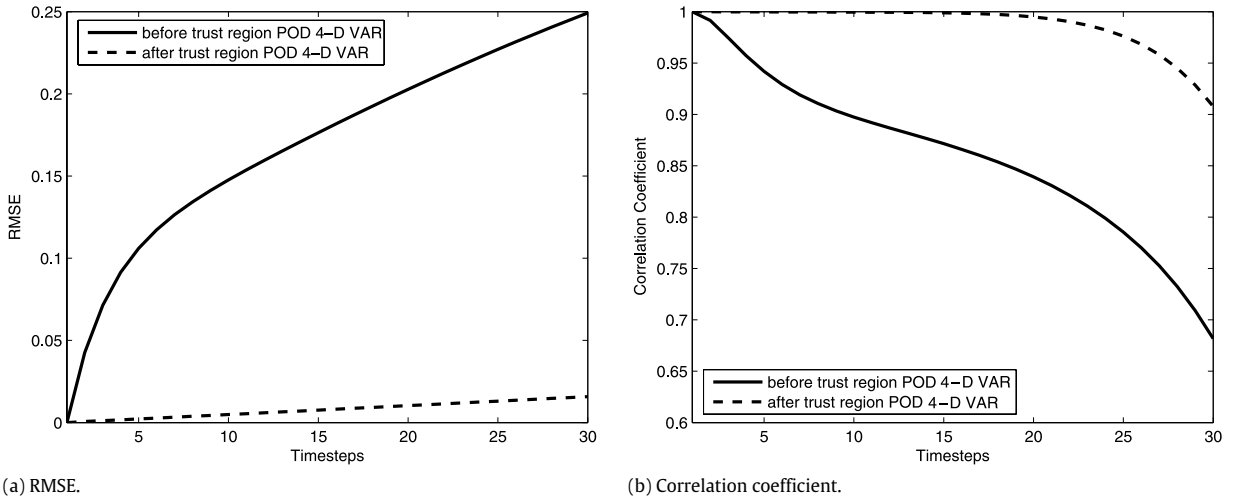


Fig. 9. Comparison of the RMSE and correlation coefficient between the full model and the POD reduced order model before and after trust region POD 4D VAR data assimilation.

Table 1
Comparison of the performance of the full 4D VAR, the POD 4D VAR, the ad-hoc adaptive POD 4D VAR and the trust region POD 4D VAR for the PNS model.

4D VAR	Full	POD	Ad-hoc adaptive POD	Trust region POD
Iterations	259	32	71	153
Outer projections	N/A	N/A	2	6
Cost functional	10^{-4}	$10^{-1.2}$	$10^{-1.5}$	$10^{-1.9}$
CPU time (s)	69.93	10.16	21.18	42.33

In the present paper, the root-mean square error (RMSE) and the correlation coefficient (COR) between the full PNS model and the POD reduced order one are defined as

$$RMSE^l = \sqrt{\frac{\sum_{i=1}^M (V_i^l - V_{0,i}^l)^2}{M}}, \quad l = 1, \dots, L \tag{5.4}$$

and

$$COR^l = \frac{\sum_{i=1}^M (V_i^l - \bar{V}^l)(V_{0,i}^l - \bar{V}_0^l)}{\sqrt{\sum_{i=1}^M (V_i^l - \bar{V}^l)^2} \sqrt{\sum_{i=1}^M (V_{0,i}^l - \bar{V}_0^l)^2}}, \quad l = 1, \dots, L \tag{5.5}$$

where V_i^l and $V_{0,i}^l$ are vectors containing the POD reduced order model solution and the full model solution of the state variables respectively, \bar{V}^l and \bar{V}_0^l are average solutions over the y direction corresponding to the POD reduced order model and the full PNS model respectively, M is the number of nodes along the y direction and L is the number of “timesteps” (the x direction).

The RMSE and correlation coefficient between the POD reduced order model and the full model before and after the trust region POD 4D VAR data assimilation are presented in Fig. 9. The results obtained show that the use of the trust region POD 4D VAR data assimilation improved the performance of the reduced order PNS model.

A summary of the performance of the full 4D VAR, the POD 4D VAR, the ad-hoc adaptive POD 4D VAR and the trust region POD 4D VAR for the reduced order inverse problem of the PNS model is provided in Table 1.

5.3. Numerical results with improved POD reduced order model

To improve the results of the trust region POD 4D VAR data assimilation process, we made some experiments on the mesh resolution and the selection of POD basis functions adopted to construct the POD reduced order model. The number of grid points along the y direction was increased from 100 to 400. The number of POD basis functions chosen to construct

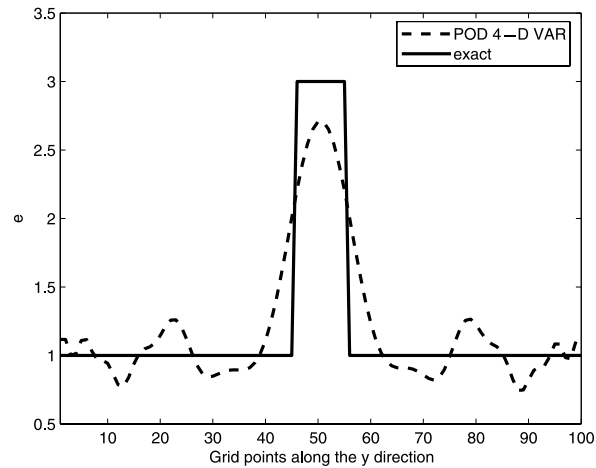


Fig. 10. The control variables at the entrance boundary for the trust region POD 4D VAR compared with the exact one.

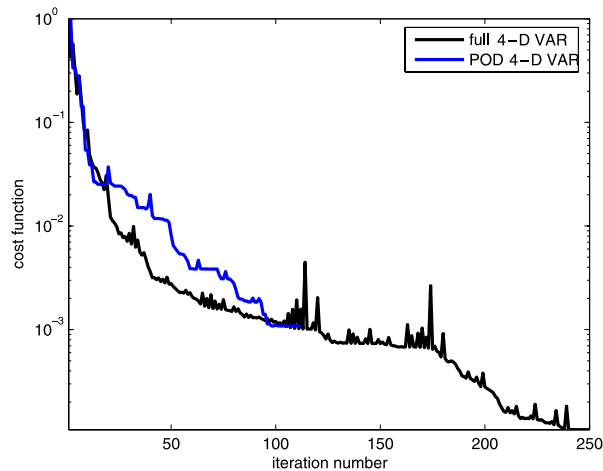


Fig. 11. The performance of minimization of the cost functional for the trust region POD 4D VAR and full 4D VAR.

the reduced order model was increased from six to thirty. When generating the POD basis functions, a H^1 norm calibration method [35] was applied using the gradient information of the snapshots.

After the improvement for the PNS reduced order model, the initial condition (control variable) for the PNS model at the entrance boundary using the trust region POD 4D VAR compared with the exact one was shown in Fig. 10. The reduction of the cost functional is shown in Fig. 11. We can see that the cost functional is reduced to 10^{-3} compared with 10^{-4} of the full 4D VAR.

The results of the full 4D VAR and trust region POD 4D VAR data assimilation are shown in Fig. 12. We can see that the result of the POD reduced order model is almost as good as that of the full order model except for some oscillations due to shortwave instability.

A summary of the performance of the full 4D VAR and the trust region POD 4D VAR for the reduced order inverse problem of the PNS model using the fine mesh and the improved POD reduced order model is provided in Table 1.

The oscillations in the POD results in the data assimilation process are due to short wave instability in the POD reduced order ordinary differential equation(ODE) system. We will focus on introducing the POD calibration using Tikhonov regularization, as well as the artificial viscosity [36,37] and mesh stretching [38,39] to get rid of the oscillations in the POD results in future work.

6. Conclusions and future work

A Proper Orthogonal Decomposition (POD) technique is applied to the ill-posed inverse problem of the parabolized Navier–Stokes (PNS) equations in order to estimate the inflow parameters from the outflow measurements of the two-dimensional supersonic laminar flow. The ad-hoc adaptive POD 4D VAR data assimilation method along with the trust region POD 4D VAR method are studied aiming to improve the performance of the reduced order model. The bound-constrained

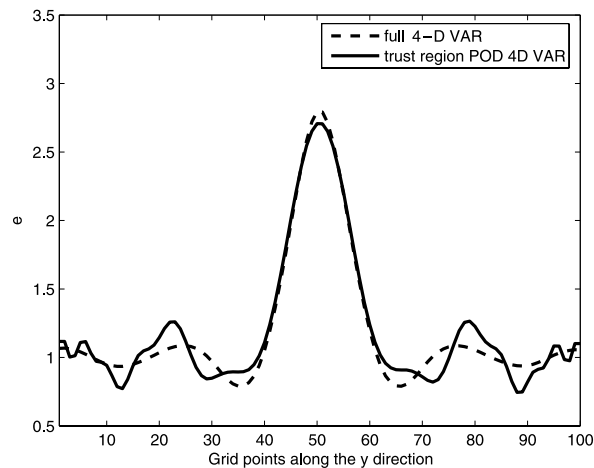


Fig. 12. The control variables at the entrance boundary for the trust region POD 4D VAR compared with full 4D VAR.

Table 2

Comparison of the performance of the full 4D VAR, the POD 4D VAR, the ad-hoc adaptive POD 4D VAR and the trust region POD 4D VAR for the PNS model.

4D VAR	Full	Trust region POD
Iterations	259	112
Outer projections	N/A	6
Cost functional	10^{-4}	10^{-3}
CPU time (s)	69.93	36.26

version of the limited-memory BFGS method is applied in the optimization process of the trust region POD 4D VAR of the PNS model. It is evident from the numerical results obtained that the trust region POD 4D VAR method obtained the best estimation of the control variables amongst all the POD adaptive methods tested, in all error metrics for the reduced order inverse problem of the PNS equations (see Table 2).

In future research we will implement the shift-mode for non-equilibrium modes proposed by Noack et al. [40–42] that may improve the results obtained by the trust region POD 4D VAR data assimilation. And we will consider applying the calibration of the POD reduced order model using the Tikhonov regularization [43] addressing the issue of the choice of a suitable parameter for the regularization using the L -curve method. Also we will focus on introducing the artificial viscosity [36,37] and mesh stretching [38,39] to get rid of the oscillations due to short wave instability in the POD reduced order model. Another approach will consist in using the bundle algorithm of non-smooth optimization coupled with the bound-constrained L-BFGS-B [44,45] to address the ill-posedness of the inverse problem in the framework of the trust region POD adaptivity.

Acknowledgments

Prof. I.M. Navon acknowledges the support of NSF grant ATM-0931198. Juan Du acknowledges the support of the China Scholarship Council and the Department of Scientific Computing that hosted her for a 1-year visit to Florida State University, FL, USA. Prof. Jiang Zhu acknowledges the support of the National Natural Science Foundation (Grant No. 41075064).

References

- [1] A.K. Alekseev, I.M. Navon, J.L. Steward, Comparison of advanced large-scale minimization algorithm for the solution of inverse ill-posed problems, *Optimization Methods and Software* 24 (2009) 63–87.
- [2] D.A. Anderson, J.C. Tannehill, R.H. Pletcher, *Computational Fluid Mechanics and Heat Transfer*, Hemisphere Publ. Corp. NY 2, 1998.
- [3] P.T.M. Vermeulen, A.W. Heemink, Model-reduced variational data assimilation, *Monthly Weather Review* 134 (2006) 2888–2899.
- [4] H.V. Ly, H.T. Tran, Proper orthogonal decomposition for flow calculations and optimal control in a horizontal CVD reactor, *Quarterly of Applied Mathematics* 60 (2002) 631–656.
- [5] O.K. Rediniotis, J. Ko, X. Yue, A.J. Kurdila, Synthetic Jets, Their Reduced Order Modeling and Applications to Flow Control, AIAA Paper number 99–1000, 37 Aerospace Sciences Meeting & Exhibit, Reno, 1999.
- [6] Y. Cao, J. Zhu, Z. Luo, I.M. Navon, Reduced order modeling of the upper tropical pacific ocean model using proper orthogonal decomposition, *Computers and Mathematics with Applications* 52 (2006) 1373–1386.
- [7] Z. Luo, R. Wang, J. Zhu, Finite difference scheme based on proper orthogonal decomposition for the non-stationary Navier–Stokes equations, *Science in China Series A: Mathematics* 50 (8) (2007) 1186–1196.
- [8] F. Fang, C.C. Pain, I.M. Navon, G.J. Gorman, M.D. Piggott, P.A. Allison, P.E. Farrell, A.J.H. Goddard, A POD reduced order unstructured mesh ocean modelling method for moderate Reynolds number flows, *Ocean Modelling* 28 (2009) 127–136.

- [9] M. Fahl, E.W. Sachs, Reduced order modelling approaches to PDE-constrained optimization based on proper orthogonal decomposition, in: Large-Scale PDE-Constrained Optimization, in: Book Series: Lecture Notes in Computational Science and Engineering, vol. 30, 2003, pp. 268–280.
- [10] S.S. Ravindran, A reduced-order approach for optimal control of fluids using proper orthogonal decomposition, *International Journal for Numerical Methods in Fluids* 34 (2000) 425–448.
- [11] M.U. Altaf, A.W. Heemink, M. Verlaan, Inverse shallow-water flow modeling using model reduction, *International Journal for Multiscale Computational Engineering* 7 (6) (2009) 577–594.
- [12] F. Fang, C.C. Pain, I.M. Navon, M.D. Piggott, G.J. Gorman, P.E. Farrell, P.A. Allison, A.J.H. Goddard, A POD reduced-order 4D-VAR adaptive mesh ocean modelling approach, *International Journal for Numerical Methods in Fluids* 60 (2009) 709–732.
- [13] Y. Cao, J. Zhu, I.M. Navon, Z. Luo, A reduced order approach to four-dimensional variational data assimilation using proper orthogonal decomposition, *International Journal for Numerical Methods in Fluids* 53 (2007) 1571–1583.
- [14] M. Bergmann, L. Cordier, Control of the circular cylinder wake by trust-region methods and POD reduced-order models, INRIA research report, 2008.
- [15] E. Arian, M. Fahl, E.W. Sachs, Trust-region proper orthogonal decomposition for flow control, Icase report 2000–25, Institute for Computer Applications in Science and Engineering, 2000.
- [16] M. Fahl, Trust-region methods for flow control based on reduced order modeling, Ph.D. Thesis, Trier University, 2000.
- [17] J. Nocedal, S.J. Wright, *Numerical Optimization*, second ed., in: Springer Series in Operations Research and Financial Engineering, Springer, New York, 2006.
- [18] M. Bergmann, L. Cordier, Optimal control of the cylinder wake in the laminar regime by trust-region methods and POD reduced-order models, *Journal of Computational Physics* 227 (2008) 7813–7840.
- [19] L. Toint, Global convergence of a class of trust-region methods for nonconvex minimization in Hilbert space, *IMA Journal of Numerical Analysis* 8 (1988) 231–252.
- [20] S.G. Rubin, J.C. Tannehill, Parabolized/reduced Navier–Stokes computational techniques, *Annual Review of Fluid Mechanics* 24 (1992) 117–144.
- [21] A.K. Alekseev, On estimation of entrance boundary parameters from downstream measurements using adjoint approach, *International Journal for Numerical Methods in Fluids* 36 (2001) 971–982.
- [22] A.K. Alekseev, I.M. Navon, The analysis of an ill-posed problem using multiscale resolution and second order adjoint techniques, *Computer Methods in Applied Mechanics and Engineering* 190 (2001) 1937–1953.
- [23] A.K. Alekseev, 2D inverse convection dominated problem for estimation of inflow parameters from outflow measurements, *Inverse Problems in Engineering* 8 (2000) 413–434.
- [24] J. Du, J. Zhu, Z. Luo, I.M. Navon, An optimizing finite difference scheme based on proper orthogonal decomposition for CVD equations, *Communications in Numerical Methods in Engineering* 27 (1) (2011) 78–94.
- [25] G.H. Golub, C.F. Van Loan, *Matrix Computations*, The Johns Hopkins University Press, Baltimore, 1990.
- [26] K. Afanasiev, M. Hinze, Adaptive control of a wake flow using proper orthogonal decomposition, in: *Shape Optimization and Optimal Design: Proceedings of the IFIP Conference*, CRC Press, 2001, pp. 317–332.
- [27] M. Hinze, K. Kunisch, Three control methods for time-dependent fluid flow, *Flow, Turbulence and Combustion* 65 (2000) 273–298.
- [28] R. Pinnau, Model reduction via proper orthogonal decomposition, in: *Model Order Reduction: Theory, Research Aspects and Applications*, Springer, 2000.
- [29] J. Blum, F.X. Le Dimet, I.M. Navon, Data assimilation for geophysical fluids, in: R. Temam, J. Tribbia (Eds.), *Computational Methods for the Atmosphere and the Oceans*, in: Special Volume of Handbook of Numerical Analysis, vol. 14, Elsevier Science Ltd., New York, 2008.
- [30] F. Bouttier, P. Courtillot, Data assimilation concepts and methods, ECMWF Meteorological Training Course Lecture Series, March 1999.
- [31] D.N. Daescu, I.M. Navon, A dual-weighted approach to order reduction in 4DVAR data assimilation, *Monthly Weather Review* 136 (3) (2008) 1026–1041.
- [32] X. Chen, I.M. Navon, F. Fang, A dual-weighted trust-region adaptive POD 4D-VAR applied to a finite-element shallow-water equations model, *International Journal for Numerical Methods in Fluids* (2009) <http://dx.doi.org/10.1002/flid.2198>. Published online in Wiley InterScience www.interscience.wiley.com.
- [33] R.H. Byrd, P. Lu, J. Nocedal, A limited memory algorithm for bound constrained optimization, *SIAM Journal on Scientific and Statistical Computing* 16 (5) (1995) 1190–1208.
- [34] C. Zhu, R.H. Byrd, J. Nocedal, L-BFGS-B: Algorithm 778: L-BFGS-B, FORTRAN routines for large scale bound constrained optimization, *ACM Transactions on Mathematical Software* 23 (4) (1997) 550–560.
- [35] J. Du, I.M. Navon, J.L. Steward, A.K. Alekseev, Reduced-order modeling based on POD of a parabolized Navier Stokes equation model I: forward model, *International Journal for Numerical Methods in Fluids* 69 (3) (2012) 710–730.
- [36] Z. Wang, I. Akhtar, J. Borggaard, T. Iliescu, Two-level discretizations of nonlinear closure models for proper orthogonal decomposition, *Journal of Computational Physics* 230 (2011) 126–146.
- [37] J. Borggaard, T. Iliescu, Z. Wang, Artificial viscosity proper orthogonal decomposition, *Mathematical and Computer Modelling* 53 (2011) 269–279.
- [38] T. Ikeda, P.A. Durbin, Mesh stretch effects on convection in flow simulations, *Journal of Computational Physics* 199 (2004) 110–125.
- [39] M.L. Rapun, J.M. Vega, Reduced order models based on local POD plus Galerkin projection, *Journal of Computational Physics* 229 (2010) 3046–3063.
- [40] B.R. Noack, K. Afanasiev, M. Morzynski, G. Tadmor, F. Thiele, A hierarchy of low-dimensional models for the transient and post-transient cylinder wake, *Journal of Fluid Mechanics* 497 (2003) 335–363.
- [41] B.R. Noack, G. Tadmor, M. Morzynski, Low-dimensional models for feedback flow control, Part I: Empirical Galerkin models, 2nd AIAA Flow Control Conference, Portland, Oregon, USA, June 28–July 1, 2004, AIAA-Paper 2004–2408 (invited contribution).
- [42] B.R. Noack, M. Schlegel, M. Morzynski, G. Tadmor, System reduction strategy for Galerkin models of fluid flows, *International Journal for Numerical Methods in Fluids* 63 (2) (2010) 231–248.
- [43] L. Cordier, B. Abou El Majd, J. Favier, Calibration of POD reduced-order models using Tikhonov regularization, *International Journal for Numerical Methods in Fluids* 63 (2010) 269–296. (Special Issue: Industrial Applications of Low-order Models Based on Proper Orthogonal Decomposition (POD), Issue Edited by Angelo Iollo, I. Michael Navon).
- [44] N. Kar Mitsa, M.M. Makela, Adaptive limited memory bundle method for bound constrained largescale nonsmooth optimization, *Optimization* 59 (6) (2010) 1–18.
- [45] N. Kar Mitsa, M.M. Makela, Limited memory bundle method for large bound constrained nonsmooth optimization: convergence analysis, *Optimization Methods and Software* 25 (2010) 895–916.